Taylor & Francis
Taylor & Francis Group

SEPARATION SCIENCE AND TECHNOLOGY

Separation Science and Technology

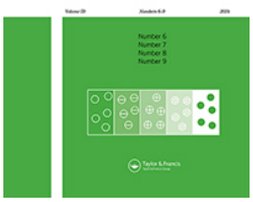

ISSN: (Print) (Online) Journal homepage: www.tandfonline.com/journals/lsst20

Green nanomaterial-based adsorbent for Cs and Pb removal: Synthesis from industrial waste producing high-value products

Juliana de Carvalho Izidoro, Amilton Barbosa Botelho Junior, Henry Tchemra Muracami, Tharcila Colachite Rodrigues Bertolini, Rebeca Piumbato Chaparro Rodrigues, Katia Silva, Miguel Gustavo Costa Ortega, Denise Alves Fungaro, Denise Crocce Romano Espinosa & Jorge Alberto Soares Tenório

To cite this article: Juliana de Carvalho Izidoro, Amilton Barbosa Botelho Junior, Henry Tchemra Muracami, Tharcila Colachite Rodrigues Bertolini, Rebeca Piumbato Chaparro Rodrigues, Katia Silva, Miguel Gustavo Costa Ortega, Denise Alves Fungaro, Denise Crocce Romano Espinosa & Jorge Alberto Soares Tenório (2024) Green nanomaterial-based adsorbent for Cs and Pb removal: Synthesis from industrial waste producing high-value products, Separation Science and Technology, 59:6-9, 909-920, DOI: 10.1080/01496395.2024.2349188

To link to this article: https://doi.org/10.1080/01496395.2024.2349188

View supplementary material

Published online: 05 May 2024.

Submit your article to this journal

Article views: 39

View related articles

View Crossmark data

Full Terms & Conditions of access and use can be found at
https://www.tandfonline.com/action/journalInformation?journalCode=lsst20

SEPARATION SCIENCE AND TECHNOLOGY
2024, VOL. 59, NOS. 6–9, 909–920
https://doi.org/10.1080/01496395.2024.2349188

Taylor & Francis
Taylor & Francis Group

Check for updates

Green nanomaterial-based adsorbent for Cs and Pb removal: Synthesis from industrial waste producing high-value products

Juliana de Carvalho Izidoro[a], Amilton Barbosa Botelho Junior[b], Henry Tchemra Muracami[a], Tharcila Colachite Rodrigues Bertolini[a], Rebeca Piumbato Chaparro Rodrigues[a], Katia Silva[a], Miguel Gustavo Costa Ortega[b], Denise Alves Fungaro[a], Denise Crocce Romano Espinosa[b], and Jorge Alberto Soares Tenório[b]

[a]Instituto de Pesquisas Energéticas e Nucleares, IPEN/CNEN, Universidade de São Paulo, São Paulo, SP, Brasil; [b]Departamento de Engenharia Química, Escola Politécnica, Universidade de São Paulo, São Paulo, Brasil

ABSTRACT

The search for a sustainable society makes necessary the reuse of residues contributing to the producing high-value product. Producing new materials with high-added value increases technological development and builds up new applications. The present study aimed to use residue from the alumina industry and coal ash generated in thermal plants in energy production to synthesize zeolite for wastewater treatment to remove Cs and Pb. Two types of nanomaterials were synthesized: zeolite 4A (ZEA) and zeolite sodalite (ZSD). The Cs adsorption efficiency achieved 73% and 9.4% for ZEA and ZSD, respectively, fitting better for Lineweaver-Burk isotherm and both zeolites removed 100% of Pb from synthetic solutions. Results here reported may be used to design novel wastewater treatment systems from nuclear plants and other industrial processes. The present study can contribute to achieving Sustainable Development Goals 9, 11, and 12.

Highlights

- Cs removal achieved 73% for ZEA fitting better for Lineweaver-Burk isotherm
- Nanozeolites were obtained from alumina industry residue
- Nanomaterials were capable to remove elements present in nuclear wastewater
- Removal of Pb achieved 100% by both zeolites

ARTICLE HISTORY
Received 18 November 2023
Accepted 24 April 2024

KEYWORDS
Aluminum residue; nanomaterials synthesis; Cs removal; Pb removal

Introduction

Aluminum is a metal of great importance to humanity because of its presence in several products, which are applied in transport areas (such as car wheels, aircraft parts, and others), beverage and food packaging, sporting goods, materials used in civil construction, household utensils, and industrial equipment. This metal is obtained from bauxite ore, which undergoes a refining process (known as the Bayer Process) to obtain alumina (Al_2O_3). Then, the alumina is converted into the primary metallic aluminum (Al) through an electrolytic process known as the Hall-Héroult process.[1]

In the secondary industry, solid residue is pre-treated to remove contaminants that could harm the process. Then, different methods can be used to recover aluminum, called "secondary aluminum." Later, recovered secondary Al is routed to product manufacturing. The portion that could not be recovered in the secondary industry can be divided into "black dross" and "salt cake," with the first portion containing from 12% to 18% recoverable aluminum and the second from 3 to 5% residual metallic aluminum.[2]

It is estimated that 200 to 500 kg of salt cake is produced per ton of secondary aluminum.[3] Black dross and salt cake can be processed in the tertiary industry (through a leaching process) to form another portion of recyclable aluminum, which returns to the secondary industry to be recycled again. The remaining waste is discharged into landfills because it has no application,[2,3] although it may have some aluminum content.

Although the aluminum industry had a metal recovery cycle that may benefit the environment, the final residue is not recycled. Thus, solid waste was chosen in this study because it still represents a challenge to be solved by the aluminum industry and an environmental problem.

CONTACT Amilton Barbosa Botelho Junior amilton.barbosa20@gmail.com Departamento de Engenharia Química, Escola Politécnica, Universidade de São Paulo, São Paulo, SP 05508-080, Brasil
Supplemental data for this article can be accessed online at https://doi.org/10.1080/01496395.2024.2349188
© 2024 Taylor & Francis Group, LLC

According to Statista (2020), Brazil recycles 98% of aluminum, while Europe and North America recycle 75% and 55%, most of them from cans.[4] However, residues generated must be better explored. Despite that, the literature reports their application in high-valuable products. Among them it may be cited the production of zeolites for wastewater or gas treatment.[5,6]

In addition to the aluminum source, the synthesis of zeolites requires a source of silicon since these two elements are a part of the basic structure of this type of material. Some industrial waste, whose main composition is silicon, can be used as raw material in the synthesis of zeolites.[7,8] Among these materials, coal ash is a highlight, and its application as a raw material for zeolite synthesis has been widely studied.[9–13] In addition, mining wastes may contain silicon and can potentially be a source for zeolite synthesis.[14,15]

Synthesis of zeolites for wastewater treatment

The most common method of synthesizing zeolite is the classical alkaline conversion using a sodium hydroxide solution in one step. This method results in a zeolitic material that contains between 20–75% of zeolite, depending on the activation reaction conditions, and the quantity of unconverted coal ash. However, because the zeolitic material is a mixture of zeolites and unconverted ash, this material cannot replace pure zeolite in all applications. Due to this restriction, a two-step activation method involving a fusion step followed by conventional hydrothermal treatment (also known as indirect conversion) was developed to improve the conversion of ash to obtain high-purity zeolites,[16–18] besides other recent synthesis improvements.[19,20]

Sodalite and 4A zeolites have been extensively studied due to the wide variety of their applications. These materials have adsorption and catalytic properties besides high cation exchange capacity. **Table S1** (Supplementary material) summarizes the main characteristics of the mentioned zeolites, and **Table S2** presents their potential applications.

Zeolite A has a structure suitable for removing several pollutants, mainly toxic metal ions, such as zinc and cadmium.[16] On the other hand, Sodalite zeolite (also known as hydroxy-sodalite) has low cation exchange capacity and surface area compared to zeolite A, but these factors do not limit the application of this product to store small molecules, such as hydrogen and radioactive effluents.[21,22]

Removing radioactive compounds from wastewater is also an issue that needs attention. For example, in 2011, the accident at the nuclear power plant in Fukushima Daiichi, Japan, was the second-worst nuclear accident in the history of nuclear power generation (due to its negative effect on the biological environment in the surrounding area). As a result, a large amount of radioactive material was released, severely contaminating water and soil. Among the various radionuclides, cesium-137 (137Cs) is considered the most worrisome due to its gamma rays' emission, one of the most abundant isotopes, long half-life (30.4 years), high water solubility, and transportability through the food chain, which makes it very dangerous for human health.[23]

The separation and removal of 137Cs from radioactive wastewater are commonly performed by different technologies, which include evaporation, solvent extraction, co-precipitation, membrane filtration, ion exchange, and adsorption.[24]

Adsorption is one of the most attractive methods for removing Cs in terms of performance of removal in a safe way, simplicity of operation, suitability for effluents with low contamination, availability of different low-cost adsorbents, and the possibility of implantation of continuous process or batch[25]

Various inorganic adsorbent materials, including zeolites, have been widely used to remove Cs^+. Literature also reports the removal of Cs^+ onto zeolite synthesized from residues.[22,26–28] The synthesis of high-purity zeolites using coal ashes has already been studied; however, the addition of an external source of aluminum is necessary to adjust the molar ratio between silicon and aluminum.[29–31] The use of aluminum residue instead of commercial did not result in high-purity products yet. Thus, using aluminum waste to obtain high-purity zeolites can contribute to reducing the costs in the synthesis process of these materials.

In addition, using industrial waste to synthesize new nanomaterials can contribute to achieving the Sustainable Development Goals (UN-SDGs). For this reason, this manuscript focused the synthesis of nanozeolites for removal of Cs and Pb. These elements can be found in nuclear plant and industrial wastewaters.[32] Indeed, several papers have reported the use of nanomaterials for wastewater treatment,[33–36] and the use of a waste material to synthesize zeolites for wastewater treatment represents a great novelty.

The novelty of this study is addressed to the application of aluminum industry waste to the synthesis of two different zeolites, contributing to the producing high-value product. The main advantage of these synthetic zeolites is the use of residue as raw material for their synthesis and further application in wastewater treatment. Sodalite and A-type zeolites were synthesized from two residues (coal ash generated in thermal plants

in energy production and industrial aluminum residue) and applied for removing Cs and Pb from simulated wastewater.

Materials and methods

Sample of solid aluminum waste

The aluminum residue sample (AR) from the tertiary industry was collected in an aluminum industry in the State of São Paulo, Brazil, in December 2015. AR residue was crushed in a mortar and pestle, washed with deionized water in the proportion of 20 g of residue to 500 mL of water, filtered, and dried at 105°C overnight. Then, the dry residue was sieved until it passed through a 0.5 mm sieve (ASTM 35). The treated aluminum residue was labeled as TAR.

Coal ash sample

The coal ash sample (CA) was collected at the Jorge Lacerda Thermoelectric Power Plant in Santa Catarina State, Brazil, in June 2015. This sample was used without any pretreatment before being used to synthesize zeolites.

Nanomaterials synthesis

Both solid wastes have the zeolites' structural elements (Si and Al) in their chemical composition; however, they are not available to synthesize the products because they are in crystalline forms, such as quartz, mullite, and corundum. Therefore, compounds must be "broken" by fusion before the hydrothermal treatment and further zeolite synthesis.[16,37] Thus, Sodalite and A zeolite synthesis had the same starting point: sodium hydroxide was grounded and mixed with both residues until a homogeneous mixture was obtained. The NaOH and the coal ash sample were mixed using the ratio of 1.2:1.0 (wt%). At the same time, the amount of the treated aluminum residue (TAR) was adjusted to follow the specific SiO_2/Al_2O_3 ratio for each type of product. The mixture was heated at 550°C for 1 h and then cooled at room temperature.

In the synthesis of sodalite zeolite, 250 mL of deionized water was added to the ground mixture. The mixture was then stirred at room temperature for 2 h and heated to 100°C for 24 h. The suspension was filtered, the solid was washed with 1 L of deionized water, and dried at 105°C overnight. The product was labeled as ZSD. In synthesizing A zeolite, 200 mL of deionized water was added to the ground sample. The suspension was stirred at room temperature for 16 h and heated to 100°C for 7 h. The product was filtered, washed, and dried at 105°C overnight as sodalite zeolite. The product was labeled as ZEA.

Industrial wastes and nanomaterials characterization

Both raw materials were characterized to determine the chemical composition by X-ray fluorescence (Panalytical Spectrometer – Axios Advanced) and mineral assessment by X-ray diffraction (XRD – Rigaku – Miniflex II, with a monochromator and Cu Kα radiation at 30kV, 15 mA, 0.05°/s and 5–80° (2θ)). The crystalline phases were identified using the ICDD powder diffraction file database and the Search-Match computer program. The morphology was analyzed with a scanning electron microscope, where each sample was placed on metallic support and covered with a thin layer of gold (SEM – HITACHI – TM3000).

The chemical composition of the synthesized nanomaterials was determined by a Zetium X-ray fluorescence spectrometer (Malvern Panalytical). The morphology was examined using a scanning electron microscope (Thermo Fisher Scientific – Quanta 650 FEG). Each sample was prepared using a metallizer Coating System (BAL-TEC – MED-020) prior to the observation in the microscope. The surface area of the zeolites was also analyzed by the Brunauer-Emmett-Teller method (BET Micrometrics ASAP 2020). Particle size distribution was analyzed (Malvern Mastersizer, 2000) to determine the granulometric distribution. An infrared spectrometer with Fourier transform (FT-IR Tensor 27 – Bruker) was used to identify the chemical bonds of the zeolites synthesized.

Adsorption experiments for pollutants removal

The experiments were carried out in batch using the zeolites previously synthesized and dried at 60°C for 24 h. For the experiments, synthetic solutions of Cs (as Cs^{+}) and Pb (as Pb^{+2}) in chlorite media were prepared, and the pH was adjusted using HCl or NaOH. The solution was mixed with the zeolite in an Erlenmeyer flask in an orbital shaker (Multitron Pro Infors HT) at 25°C and 200 rpm for 2 h. After the experiment, the mixture was filtered using filter paper (2 μm), and the solution was analyzed in ICP-OES (Agilent Technologies 70 series) which the calibration curves were prepared using standard solutions proper for chemical analysis. If necessary, the solution was diluted with HCl 3%.

This study evaluated the amount of zeolite, concentration of Cs and Pb, and pH. Due to the differences in adsorption efficiency for each case obtained in experimental results, the amount of zeolite was different for Cs and Pb, as depicted in **Table S3**. The experiments were carried out with 50 mL of solution.

Equation 1 was used to calculate the percentage of element adsorbed by the zeolite (%*S*), where C_0 and C_t (mg/L) are the liquid phase concentrations of solutes at the initial and given time *t*. Equation 2 was used to determine the amount of element adsorbed per mass of zeolite, where q_t (mg/g) is the equilibrium adsorption capacity, *v* is the volume of solution (L), and *m* is the weight of zeolite (g).[38–40] **Table S4** presents the isotherm models used in the present study and their respective linear equation. The present study evaluated the Langmuir, Lineweaver-Burk, Eadie-Hofstee, Scatchard, and Freundlich models.[41]

$$\%S = \frac{(C_0 - C_t)}{C_0} x100\% \quad (1)$$

$$q_t = (C_0 - C_t) x \frac{v}{m} \quad (2)$$

Results and discussion

Characterization of raw materials

The chemical composition of aluminum residue (AR), treated aluminum residue (TAR), and coal ash (CA) are given in **Table S4** (*Supplementary Material*). According to the results, Al is the principal constituent of AR and TAR. However, the amount of Al can vary depending on the melting process used in the industrial metal recovery. Usually, KCl and NaCl are added to the mixture to recover the metallic Al. Thus, the residue with a higher quantity of salts presents smaller amounts of Al.[42]

Table S4 also shows that the treated aluminum residue has more Al and Si than the Al residue without treatment. Therefore, TAR sample could contribute to the higher availability of these structural elements for the formation of zeolites. The Al content was highlighted as it increased from 27.8% in the raw waste to 73.2% in the treated Al waste. Similarly, Cl content, which could negatively interfere with the synthesis of zeolites, had its content decreased from 17.4% in the AR sample to 0.41% in the TAR sample. This result was confirmed by the XRD analysis where the NaCl peaks in the raw residue were no longer present in the treated residue (**Figure S1**).

Therefore, results indicate that TAR has the potential to be a better source to synthesize zeolites than AR. Elements such as Ca, Fe, K, Mg, and others showed contents below 6% in both Al residues, raw and treated. The coal ash presented as main elements Si (52.6%) and Al (23.5%). The other components presented quantities below 8%.

The XRD pattern of AR shows that this sample is a complex mixture of crystalline phases formed by NaCl, KCl, $MgAl_2O_4$, Al_2O_3, and Fe_2SiO_4. The results follow an Al residue sample characterized by Shinzato & Hypolito (2004).[43] The mineralogical composition of this residue can be related to the different heat treatments that this type of sample undergoes in the recycling process.[42] NaCl is incorporated into the residue for melting process in the furnaces and it is present in the slag from the secondary industries; therefore, a large amount of NaCl can be observed in the AR sample, in addition to the aluminum phase (Al_2O_3).

For comparison, the crystalline phases of treated aluminum residue (TAR) and RA sample are shown in **Figure S3**. According to the results, treating the residue with water significantly decreased NaCl and KCl (very soluble salts). At the same time, the compounds of Mg, Al, and Fe did not show significant variations. The reduction of NaCl can be seen clearly at the angle of 75° 2θ.

The coal ash XRD pattern (**Figure S2**) shows that quartz and mullite are the main phases of the sample, in addition to hematite and magnetite, as previous reported.[16]

The SEM images of CA, AR, and TAR presented in **Figure S4** shows that the main difference between the coal ash sample and the Al residue samples is that CA presents some spherical particles, usually found for the remaining particles of the coal combustion process, while the Al residues do not present uniformity in the shape of the particles that compose them.

Characterization of nanomaterials

The chemical compositions of the synthesized nanomaterials (zeolite sodalite – ZSD, and zeolite A – ZEA) are given in Table 1. According to the results, the samples presented in general high contents of Si, Al, and Na oxide, which are the forming components of zeolites identified by XRD. Impurities such as Ca, Mg, Ti, and K presented contents below 6%.

The main phases of the nanomaterials formed after the synthesis process were identified and presented in

Table 1. Composition (wt%) of sodalite zeolite (ZSD) and zeolite a (ZEA).

Components	ZSD	ZEA
Al_2O_3	23.5	36.5
SiO_2	25.7	29.0
Na_2O	23.9	5.61
CaO	4.57	5.07
MgO	0.92	1.93
TiO_2	0.75	1.09
Fe_2O_3	4.04	5.73
K_2O	1.52	0.95
SO_3	0.58	0.08
Cl	0.09	-
Others	0.73	1.34
LOI	13.7	12.7

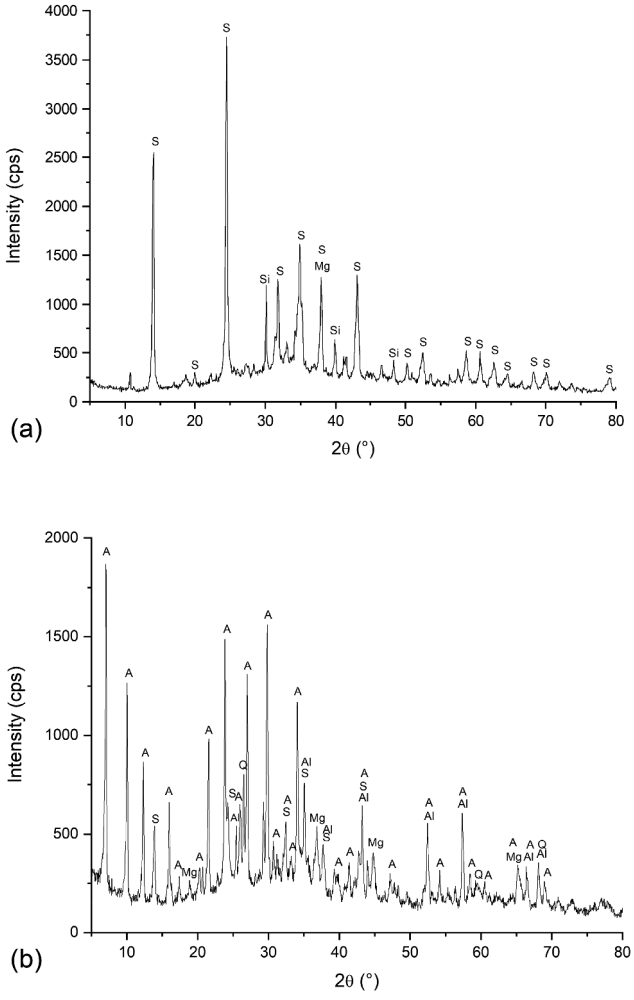

Figure 1. XRD patterns of the (a) zeolite sodalite and (b) zeolite a synthesized from coal ash and aluminum residue synthesized from coal ash and aluminum residue – (a) S = zeolite sodalite – $Na_8Al_6Si_6O_{24}(OH)_2(H_2O)_2$, Si = silicon dioxide – SiO_2, and Mg = spinel - $MgAl_2O_4$; (b) a = zeolite a – $Na_2Al_2Si_{1.85}O_{7.75}.H_2O$, Q = quartz – SiO_2, and Al = corundum - Al_2O_3.

Fig. 1a for ZSD and Fig. 1b for ZEA samples. In addition to the main phases, some compounds found in the precursor materials, such as SiO_2, spinel, and corundum, also were identified in smaller amounts. It was verified through the synthesis conditions that a more extended period of hydrothermal conditions favors the formation of the sodalite zeolite structure, which is more compact and more stable. On the other hand, zeolite A, a more porous material, formed about 1/3 of the time compared to zeolite sodalite.

The SEM micrographs of ZSD and zeolite type A ZEA were presented in Figs. 2 and 3, respectively. Sodalite zeolite presents a structure with agglomerates of particles similar to wool balls.[9,44,45] Zeolite A, on the other hand, has a characteristic cubic structure.[15,16,29] According to the images, the high purity sodalite and A zeolites can be seen and are compatible with the formats described in the cited literature.

Figure 2 shows that sodalite zeolites showed regular crystal structures of similar sizes. On the other hand, Fig. 3 shows that the characteristic cubes of zeolite A presented crystals of varying sizes. The same zeolite type may have different crystal sizes due to the difference in their growth rate during hydrothermal treatment.[29] This may have been caused by the difference in the content of the amorphous and crystalline phases of the precursor materials.[16]

BET surface analysis was carried out for both prepared zeolites, and it was obtained 3.97 m^2/g for ZEA (Langmuir surface area 5.91 m^2/g) and 9.62 m^2/g for ZSD (Langmuir surface area 10.97 m^2/g). Particle size distribution was determined and shown in **Figure S5** where the d10 and d50 were 3.38 µm and 23.92 µm for ZEA and 8.33 µm and 40.66 µm for ZSD, respectively. The FTIR analysis is depicted in **Figure S6**, where the main peaks for ZEA were 464 cm^{-1}, 557 cm^{-1}, 989 cm^{-1}, and 1386 cm^{-1}, and for ZSD were 432 cm^{-1}, 1001 cm^{-1}, and 1461 cm^{-1}.

Adsorption experiments for pollutants removal

Cs and Pb removal

The zeolites ZSD and ZEA were evaluated for the adsorption of Cs ions in chloride media varying the concentration from 0.03 g to 1.2 g with 50 mL of solution (100 mg/L Cs) at 25°C and pH 6.0 for 2 h and 200rpm. The results are presented in Fig. 4. The adsorption of Cs ions by ZEA slightly increased from 0.03 g (7.4%) to 0.40 g (9.7%). However, it reached 64.4% using 0.6 g-1.2 g since the mass of zeolite increase provided greater surface area in contact with the Cs ions and more available sites for adsorption. On the other hand, the adsorption

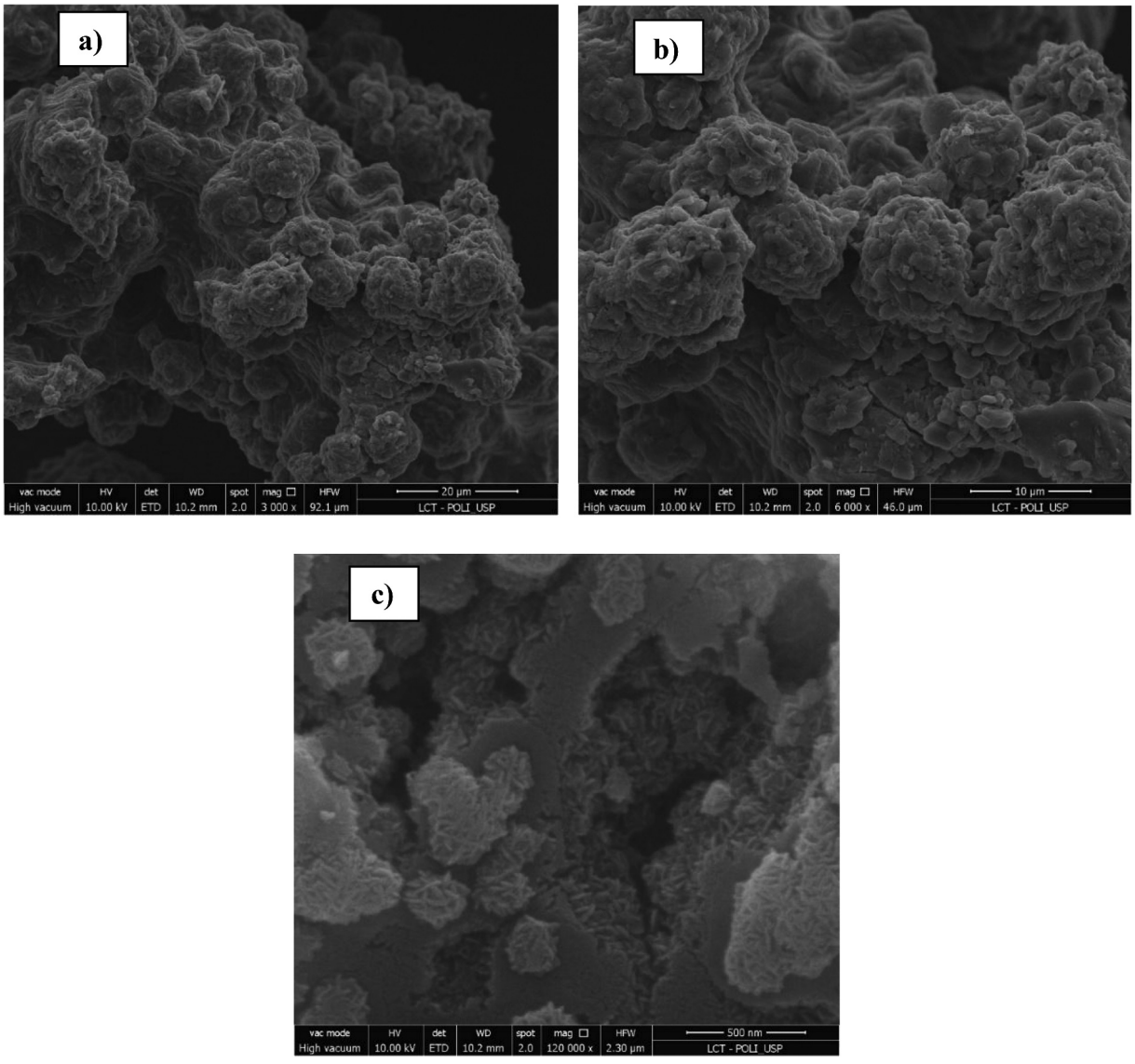

Figure 2. SEM micrograph of sodalite zeolite synthesized from industrial solid wastes (ZSD): a) 3,000x; b) 6,000x, and c) 120,000x.

capacity declined as there was more zeolite mass per Cs ions (mg Cs ions/g zeolite).[46]

In the case of ZSD, the adsorption of Cs ions was lower than 9.3% with 0.02 g and declined as the amount of zeolite increased, achieving 1.0% with 1.2 g. The adsorption capacity followed the same behavior as ZEA. For this reason, 0.6 g was adopted as the best mass of zeolite for both ZSD and ZEA.

The increase of adsorbent in the batch process would increase the adsorption of ions due to an increase in available sites.[15,39] However, as observed, the opposite was observed. The decrease of removal efficiency with the increase in the adsorbent dosage can be attributed to particle interactions, such as aggregation or agglomeration. It results in a decrease in the total surface area available to the pollutants and an increase in diffusion path length.[47] Particle interaction may also desorb some adsorbates that are only loosely and reversibly bound to the adsorbent surface.[48] Such behavior was observed in the adsorption of Na ions on natural zeolite.[49]

The Pb adsorption by the zeolites was also studied in chloride media. Figure 5 presents the adsorption efficiency and adsorption capacity varying the amount of zeolite at pH 6.0 and 25°C for 2 h. The removal of Pb ions by ZEA increased from 0% (0.005 g-0.5 g) to 7.8% (0.1 g) and 78% (0.2 g) and achieved 100% with 0.3 g. It occurs because more active sites are available for the adsorption

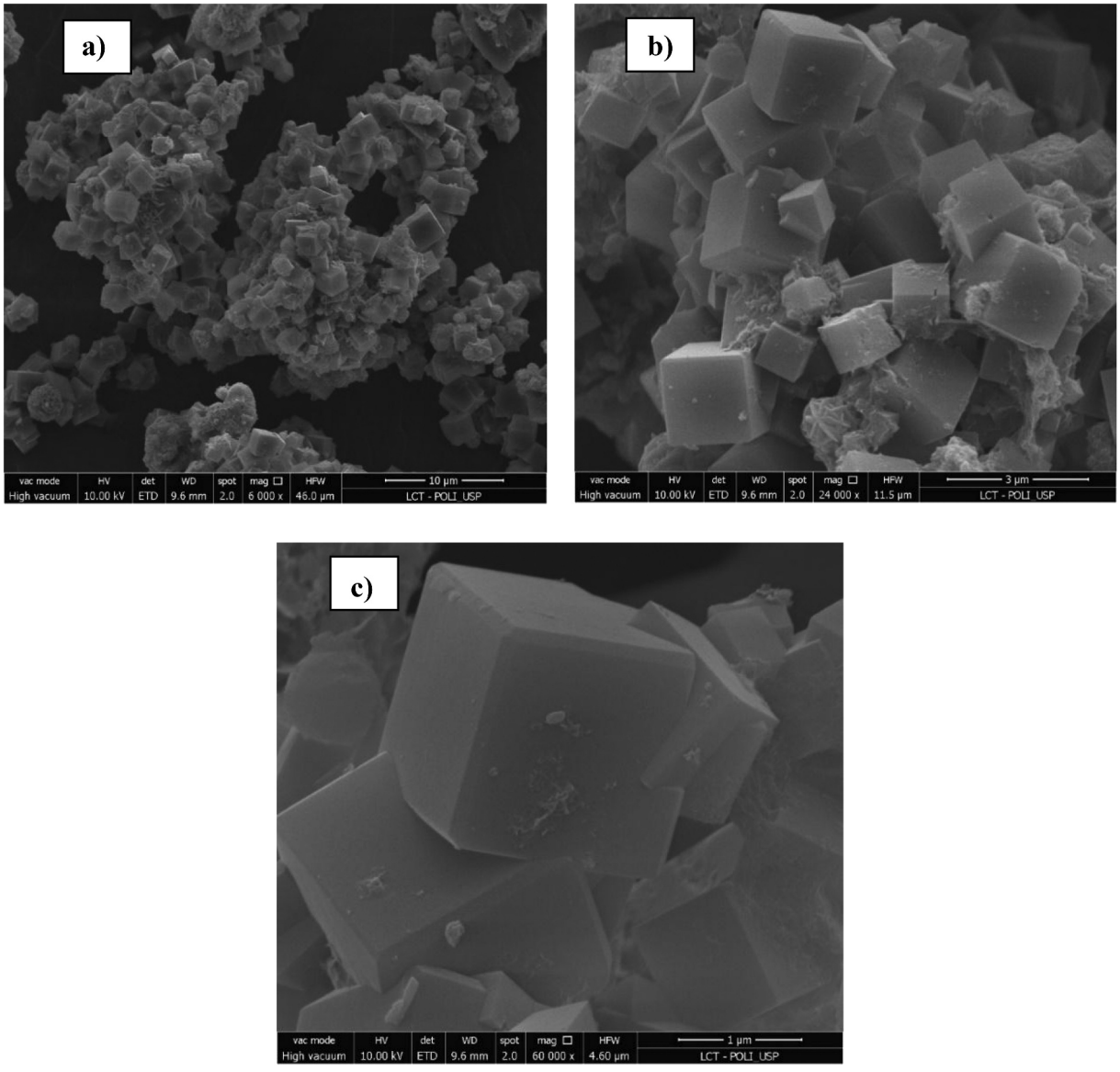

Figure 3. SEM micrograph of zeolite a synthesized from industrial solid wastes (ZEA): a) 6,000x; b) 24000x, and c) 600,000x.

of Pb ions, as observed from ZSD experiments.[50] Figure 5b shows the adsorption capacity, which achieved the plateau for both zeolites with 0.2 g.

The effect of Cs concentration was evaluated from 10 mg/L to 100 mg/L. The experiments were carried out at pH 6.0 and 25°C within 2 h, and the results are depicted in Fig. 6. The removal of Cs by ZEA remained almost the same as the concentration increased. In an experiment with 10 mg/L of Cs, the adsorption was 66.7% (4.9 mg Cs/g ZEA) and increased to 73.3% (59.4 mg Cs/g ZEA) in 100 mg/L Cs solution. It indicates that the concentration difference from 10 to 100 mg/L does not affect the ions' adsorption. The adsorption capacity (Fig. 6b) demonstrated a linear behavior of Cs ions.

In the case of ZSD, the adsorption achieved 32.7% from solution with 10 mg/L, and then declined to 16.9% (20 mg/L) and 2.6% (40 mg/L), and achieved 0% for concentrations higher than 60 mg/L. The adsorption capacity of ZSD from 10 mg/L to 100 mg/L varied from 2.6 mg/g to 0 mg/g, as previously discussed. The effect of Pb concentration in adsorption efficiency was evaluated from 10 mg/L to 100 mg/L, where all Pb ions were adsorbed regardless of the concentration studied for both zeolites.

The effect of pH was evaluated from 2 to 12, and the results are shown in **Table S5**. The adsorption of Cs by ZEA slightly decreased from pH 2 (67.2%) to pH 12 (61.4%). In the case of ZSD, the removal

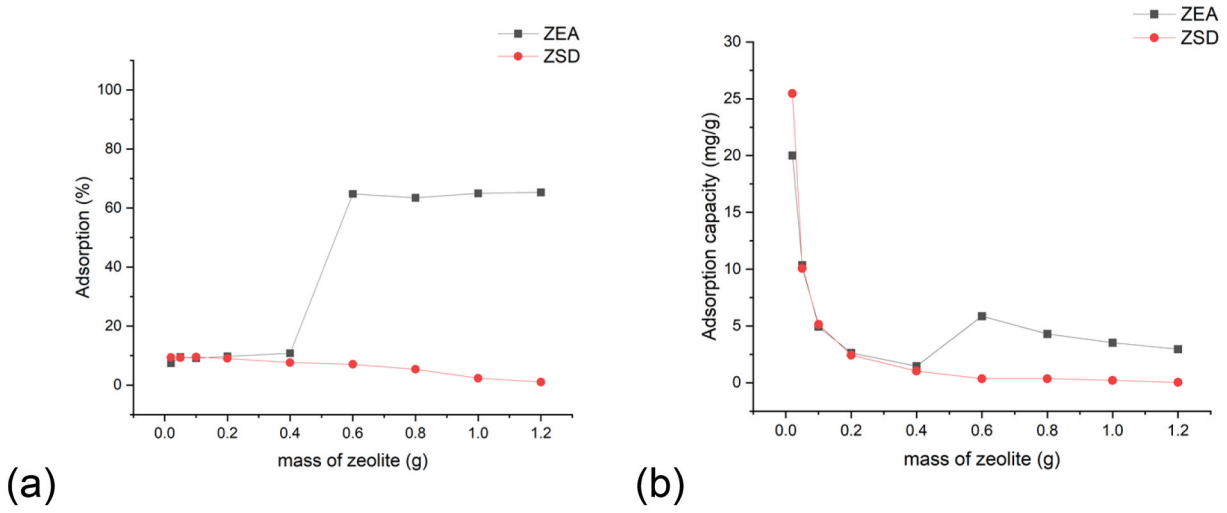

Figure 4. (a) Adsorption efficiency and (b) adsorption capacity of Cs in chloride media by ZEA and ZSD synthesized from aluminum industry waste varying the amount of zeolite. Experimental conditions: Cs concentration = 100mg/L; pH 6.0; 25°C; 200rpm; 2h.

of Cs from the solution remained lower than 1.3% and increased, achieving 5.3% at pH 12. The effect of pH was evaluated from 0.5 to 12.0. At pH 0.5, the adsorption of Pb ions was zero using both zeolites and increased to 100% at pH 2.0 and remained in this value until pH 12.0, while the Cs adsorption remained constant at around 70% for ZEA. For this reason, the data for Pb extraction is not presented graphically. It demonstrated that the decrease in the H^+ ions concentration has no influence on adsorption efficiency.[51]

Isotherm modeling

Kinetic modeling was carried out following the linear equations presented in **Table S4**. The isotherms were calculated with the data obtained varying the ions concentration. Due to the results previously presented, the modeling was carried out for Cs adsorption, as all Pb ions were adsorbed by the zeolites regardless of the concentration. The results are presented in **Table S6**, depicting that the adsorption of Cs did not fit the Langmuir, Eadie-Hofstee, and Scatchard models which the correlation coefficient (R^2) was low.

The isotherms Lineweaver-Burk and Freundlich reached R^2 equal to 0.9996 and 0.9922. It was calculated as the maximum capacity of adsorbed ions per mass of adsorbent equals 222.22 mg of Cs per g of ZEA. The adsorption energy and the equilibrium constant equal 0.01 L/mg. The Freundlich constant was determined as 1.18, and *n* (constant related to surface heterogeneity) equals 0.33.

Table 2 presents the literature review of Cs and Pb adsorption using different materials, including nanoparticles. As depicted, zeolite A has the highest

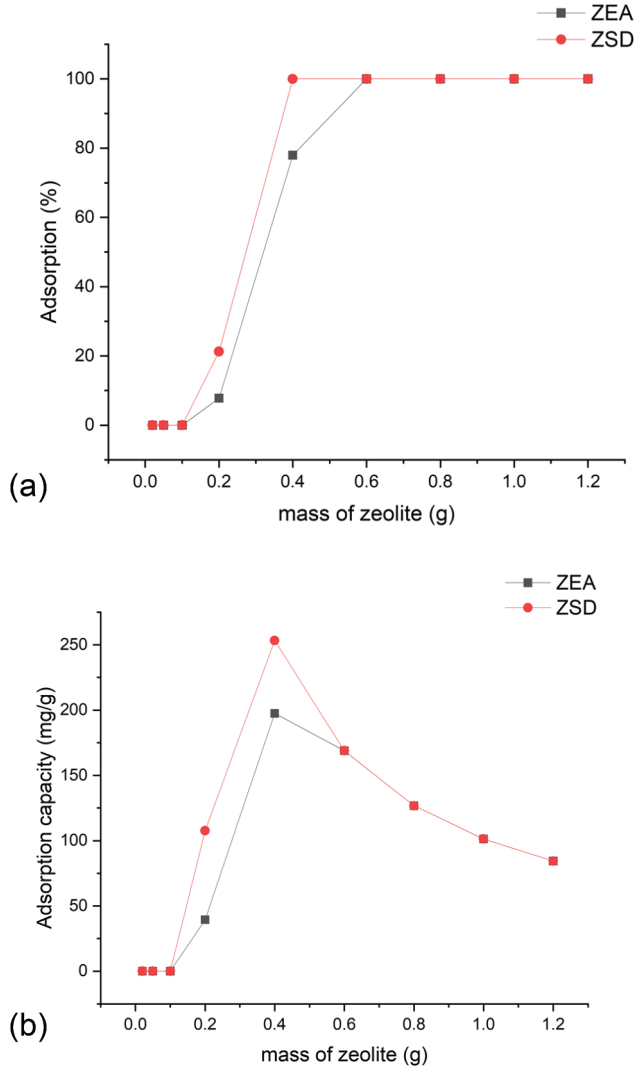

Figure 5. (a) Adsorption efficiency and (b) adsorption capacity of Pb in chloride media by ZEA and ZSD synthesized from aluminum industry waste varying the amount of zeolite. Experimental conditions: Pb concentration = 100mg/L; pH 6.0; 25°C; 200rpm; 2h.

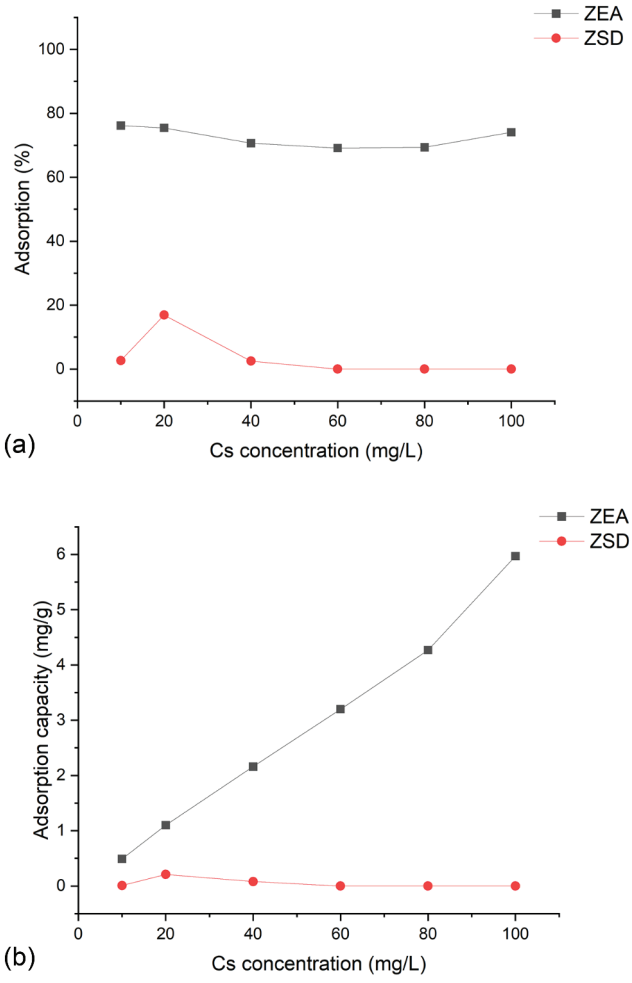

Figure 6. (a) Adsorption efficiency and (b) adsorption capacity of Cs in chloride media by ZEA and ZSD synthesized from aluminum industry waste varying the Cs concentration. Experimental conditions: mass of zeolite = 0.6g; pH 6.0; 25°C; 200rpm; 2h.

adsorption capacity among all materials herein reported (222 mg/g). Regarding Pb removal, all studies presented in Table 2 obtained 100% of ions removal from the aqueous solution. Therefore, the results obtained for both zeolites produced from an industrial residue are in accordance with the literature reaching best adsorption capacities. Future studies would focus on reuse capacity of zeolites for both Pb and Cs adsorption and application in real wastewater solution.

The use of aluminum waste and the remaining ash from the burning of coal to obtain new materials, in addition to the application in the removal of toxic compounds, such as Cs and Pb, can contribute to the achievement of the SDGs 9, 11, and 12.[14,41,57,58] It is suggested for future applications the use elution process to desorb Cs and Pb from the zeolite for final disposal and consequently recycle of the zeolites.

Conclusion

The present study aimed at synthesizing zeolites from industrial waste and application in wastewater treatment. From the results obtained, it may conclude that the treated aluminum residue from the Al industry (TAR) and the coal ash residue generated from power plants (CA) are good sources of Al and Si, respectively, for the synthesis of zeolites. The methodology used in this study was suitable for synthesizing nanomaterials and can be used from different industrial residues, confirmed by chemical and physical analysis. Batch experiments

Table 2. Literature review for Cs and Pb removal using different adsorbent materials.

Reference	Adsorbant material	Ions adsorption	Best conditions	Efficiency	Adsorption capacity	Isotherm modeling
This work	Zeolite A	Cs, Pb	Cs – 1.2g of zeolite, pH 6, 200rpm, 25°C Pb – 0.6g of zeolite, pH 6, 200rpm, 25°C	Cs – 73% Pb – 100%	Cs – 2.95mg/g Pb – 198mg/g	Lineweaver-Burk
This work	Zeolite sodalite	Cs, Pb	Cs – 0.1g of zeolite, pH 6, 200rpm, 25°C Pb – 0.6g of zeolite, pH 6, 200rpm, 25°C	Cs – 9.4% Pb – 100%	Cs – 0.04mg/g Pb – 253mg/g	Lineweaver-Burk
[52]	Mesoporous conjugated adsorbent	Pb	20mg of adsorbent, pH 5.5	100%	192mg/g	Langmuir
[53]	Ni-ZnO nanoparticles	Pb	25mg of nanoparticle, pH 5.0, 25°C	100%	69mg/g	Langmuir
[54]	Co_3O_4 co-doped TiO2nanoparticles	Pb	25mg of nanoparticle, pH 5.0, 1h	–	114mg/g	Langmuir
[55]	ZrTiPO4	Cs	50mg of adsorbent, pH 4.2, 10min, room temperature,	98.80%	51mg/g	Sips
[56]	AMP@PDA@Fe3O4 composite	Cs	120min, pH 6.0–8.0, 25–55°C	91%	38mg/g	Langmuir

demonstrated high adsorption of Cs and Pb ions, achieving a maximum of 73% and 100% by the zeolites, respectively. Adsorption of Cs achieved 73% using 1.2 g of ZEA and 9.4% using 0.1 g of ZSD at pH 6, at 25°C and 200 rpm for 2 h. In the case of Pb adsorption, both zeolites achieved 100% removal using 0.6 g of material. Cs adsorption fitted better for Lineweaver-Burk isotherm with R^2 equal to 0.9996, where the maximum capacity calculated was 222.22 mg of Cs per g of ZEA and the adsorption energy and the equilibrium constant equals 0.01 L/mg.

Acknowledgments

The authors would like to acknowledge the Fundação de Amparo à Pesquisa do Estado de São Paulo and Capes (grants: 2018/03483-6, 2019/11866-5, 2021/14842-0, 2023/01032-5 São Paulo Research Foundation) and IPEN for the financial support. This project was developed with the support of SemeAd (FEAUSP), FIA Fundação Instituto de Administração and Cactvs Instituto de Pagamento S. A. through the granting of assistance to a research project Bolsa SemeAd PQ Jr (Public Notice 2021.01).

Disclosure statement

No potential conflict of interest was reported by the author(s).

Funding

The work was supported by the Fundacao de Amparo a Pesquisa do Estado de Sao Paulo [2019/11866-5]; Fundacao de Amparo a Pesquisa do Estado de Sao Paulo [2023/01032-5]; Fundacao de Amparo a Pesquisa do Estado de Sao Paulo [2021/14842-0]; Fundacao de Amparo a Pesquisa do Estado de Sao Paulo [2018/03483-6].

ORCID

Amilton Barbosa Botelho Junior http://orcid.org/0000-0002-3421-6286

Data and code availability

The data can be accessed by https://doi.org/10.6084/m9.figshare.24152184.v1.

References

[1] Lumley, R. *Fundamentals of Aluminium Metallurgy*, 1st ed.; Woodhead Publishing: Cambridge, 2011.
[2] Satish Reddy, M.; Neeraja, D. Aluminum Residue Waste for Possible Utilisation As a Material: A Review. *Sadhana - Academy Proceedings in Engineering Sciences*. 2018, *43*:1–8, doi:10.1007/s12046-018-0866-2.
[3] Tsakiridis, P. E. Aluminium Salt Slag Characterization and Utilization - a Review. *J. Hazard. Mater*. 2012, *217–218*, 1–10. DOI: 10.1016/j.jhazmat.2012.03.052.
[4] Garside, M. Recycling Rate of Metals and Glass Worldwide Between 2015 and 2017, by Region. https://www.statista.com/statistics/1106333/global-recycling-rate-of-permanent-materials-by-region/ (accessed Feb 7, 2020).
[5] Sánchez-Hernández, R.; Padilla, I.; López-Andrés, S.; López-Delgado, A. Eco-Friendly Bench-Scale Zeolitization of an Al-Containing Waste into Gismondine-Type Zeolite Under Effluent Recycling. *J. Clean. Prod*. 2017, *161*, 792–802. DOI: 10.1016/j.jclepro.2017.05.201.
[6] Sánchez-Hernández, R.; López-Delgado, A.; Padilla, I.; Galindo, R.; López-Andrés, S. One-Step Synthesis of NaP1, SOD and ANA from a Hazardous Aluminum Solid Waste. *Micro. Mesoporous Mater*. 2016, *226*, 267–277. DOI: 10.1016/j.micromeso.2016.01.037.
[7] Gao, S.; Peng, H.; Song, B.; Zhang, J.; Wu, W.; Vaughan, J.; Zardo, P.; Vogrin, J.; Tulloch, S.; Zhu, Z. Synthesis of Zeolites from Low-Cost Feeds and Its Sustainable Environmental Applications. *J. Environ. Chem. Eng*. 2023, *11*, 108995. DOI: 10.1016/j.jece.2022.108995.
[8] Yamaura, M.; Fungaro, D. A. Synthesis and Characterization of Magnetic Adsorbent Prepared by Magnetite Nanoparticles and Zeolite from Coal Fly Ash. *J. Mater. Sci*. 2013, *48*(14), 5093–5101. DOI: 10.1007/s10853-013-7297-6.
[9] Izidoro, J. D. C.; Fungaro, D. A.; Dos Santos, F. S.; Wang, S. Characteristics of Brazilian Coal Fly Ashes and Their Synthesized Zeolites. *Fuel Process. Technol*. 2012, *97*, 38–44. DOI: 10.1016/j.fuproc.2012.01.009.
[10] Yao, Z. T.; Ji, X. S.; Sarker, P. K.; Tang, J. H.; Ge, L. Q.; Xia, M. S.; Xi, Y. Q. A Comprehensive Review on the Applications of Coal Fly Ash. *Earth Sci. Rev*. 2015, *141*, 105–121. DOI: 10.1016/j.earscirev.2014.11.016.
[11] Liu, R. Y.; Zou, L. X.; Huang, Q.; Cao, X. ChuoYang Synthesis of Analcime from Fly Ash and Its Adsorption of Cs+ in Aqueous Solution. *J. Radioanal. Nucl. Chem*. 2021, *329*(1), 103–113. DOI: 10.1007/s10967-021-07799-5.
[12] Choi, J.-H.; Lee, C.-H. Evaluation of Sr and Cs Ions Adsorption Capacities with Zeolitic Materials Synthesized from Various Mass Ratios of NaOH to Coal Fly Ash. *Environ. Eng. Res*. 2021, *27*(2), 200662–0. DOI: 10.4491/eer.2020.662.
[13] Kumar, M. M.; Jena, H. Direct Single-Step Synthesis of Phase Pure Zeolite Na–P1, Hydroxy Sodalite and Analcime from Coal Fly Ash and Assessment of Their Cs+ and Sr2+ Removal Efficiencies. *Micro. Mesoporous Mater*. 2022, *333*, 111738. DOI: 10.1016/j.micromeso.2022.111738.
[14] Botelho Junior, A. B.; Espinosa, D. C. R.; Tenório, J. A. S. Extraction of Scandium from Critical Elements-Bearing Mining Waste: Silica Gel Avoiding in Leaching Reaction of Bauxite Residue. *J. Sustainable Metall*. 2021, *7*(4), 1627–1642. DOI: 10.1007/s40831-021-00434-3.

[15] Izidoro, J. C.; Kim, M. C.; Bellelli, V. F.; Pane, M. C.; Botelho Junior, A. B.; Espinosa, D. C. R.; Tenório, J. A. S. Synthesis of Zeolite a Using the Waste of Iron Mine Tailings Dam and Its Application for Industrial Effluent Treatment. *J. Sust. Mining*. 2019, *18*, 277–286. DOI: 10.1016/j.jsm.2019.11.001.

[16] Izidoro, J. D. C.; Fungaro, D. A.; Abbott, J. E.; Wang, S. Synthesis of Zeolites X and a from Fly Ashes for Cadmium and Zinc Removal from Aqueous Solutions in Single and Binary Ion Systems. *Fuel*. 2013, *103*, 827–834. DOI: 10.1016/j.fuel.2012.07.060.

[17] Kazemian, H.; Naghdali, Z.; Ghaffari Kashani, T.; Farhadi, F. Conversion of High Silicon Fly Ash to Na-P1 Zeolite: Alkaline Fusion Followed by Hydrothermal Crystallization. *Adv. Powder Tech*. 2010, *21*(3), 279–283. DOI: 10.1016/j.apt.2009.12.005.

[18] Zhang, X.; Li, C.; Zheng, S.; Di, Y.; Sun, Z. A Review of the Synthesis and Application of Zeolites from Coal-Based Solid Wastes. *Int. J. Miner. Metall. Mater*. 2022, *29*(1), 1–21. DOI: 10.1007/s12613-021-2256-8.

[19] Chen, W.; Song, G.; Lin, Y.; Qiao, J.; Wu, T.; Yi, X.; Kawi, S. Synthesis and Catalytic Performance of Linde-Type a Zeolite (LTA) from Coal Fly Ash Utilizing Microwave and Ultrasound Collaborative Activation Method. *Catal. Today*. 2022, *397–399*, 407–418. DOI: 10.1016/j.cattod.2021.07.022.

[20] Zhao, M.; Ma, X.; Chen, D.; Liao, Y. Preparation of Honeycomb-Structured Activated Carbon–Zeolite Composites from Modified Fly Ash and the Adsorptive Removal of Pb(ii). *ACS Omega*. 2022, *7* (11), 9684–9689. DOI: 10.1021/acsomega.1c07192.

[21] Derkowski, A.; Franus, W.; Beran, E.; Czímerová, A. Properties and Potential Applications of Zeolitic Materials Produced from Fly Ash Using Simple Method of Synthesis. *Powder Tech*. 2006, *166*, 47–54. DOI: 10.1016/j.powtec.2006.05.004.

[22] Boycheva, S. V Synthetic Zeolitic Ion-Exchangers from Coal Ash for Decontamination of Nuclear Wastewaters. *BgNS Trans*. 2016, *20*, 132–136.

[23] Gonze, M. A.; Calmon, P.; Hurtevent, P.; Coppin, F. Meta-Analysis of Radiocesium Contamination Data in Japanese Cedar and Cypress Forests Over the Period 2011–2017. *Sci. Total Environ*. 2021, *750*, 142311. DOI: 10.1016/j.scitotenv.2020.142311.

[24] Hasan, M. N.; Shenashen, M. A.; Hasan, M. M.; Znad, H.; Awual, M. R. Assessing of Cesium Removal from Wastewater Using Functionalized Wood Cellulosic Adsorbent. *Chemosphere*. 2021, *270*, 128668. DOI: 10.1016/j.chemosphere.2020.128668.

[25] Khandaker, S.; Toyohara, Y.; Kamida, S.; Kuba, T. Adsorptive Removal of Cesium from Aqueous Solution Using Oxidized Bamboo Charcoal. *Water Resour. Ind*. 2018, *19*, 35–46. DOI: 10.1016/j.wri.2018.01.001.

[26] Fungaro, D. A.; Grosche, L. C.; de C Izidoro, J. Synthesis of Calcium Silicate Hydrate Compounds from Wet Flue Gas Desulfurization (FGD) Waste. *J. Appl. Mat. Tech*. 2020, *1*(2), 88–95. DOI: 10.31258/Jamt.1.2.88-95.

[27] Lalhmunsiama; Kim, J. G.; Choi, S. S.; Lee, S. M. Recent Advances in Adsorption Removal of Cesium from Aquatic Environment. *Appl. Chem. Engi*. 2018, *29*, 127–137. DOI: 10.14478/ace.2018.1019.

[28] Sterba, J. H.; Sperrer, H.; Wallenko, F.; Welch, J. M. Adsorption Characteristics of a Clinoptilolite-Rich Zeolite Compound for Sr and Cs. *J. Radioanal. Nucl. Chem*. 2018, *318*(1), 267–270. DOI: 10.1007/s10967-018-6096-6.

[29] Wang, C. F.; Li, J. S.; Wang, L. J.; Sun, X. Y. Influence of NaOH Concentrations on Synthesis of Pure-Form Zeolite a from Fly Ash Using Two-Stage Method. *J. Hazard. Mater*. 2008, *155*, 58–64. DOI: 10.1016/j.jhazmat.2007.11.028.

[30] Lee, K. M.; Jo, Y. M. Synthesis of Zeolite from Waste Fly Ash for Adsorption of CO2. *J. Mater. Cycles Waste Manag*. 2010, *12*(3), 212–219. DOI: 10.1007/s10163-010-0290-0.

[31] Izidoro, J.; Castanho, D.; Rossati, C.; Fungaro, D.; Guilhen, S.; Nogueira, T.; Fátima Andrade, M. De Application of High-Purity Zeolite a Synthesized from Different Coal Combustion By-Products in Carbon Dioxide Capture. *Int. J. EI*. 2019, *2*(3), 215–228. DOI: 10.2495/ei-v2-n3-215-228.

[32] Kadadou, D.; Said, E. A.; Ajaj, R.; Hasan, S. W. Research Advances in Nuclear Wastewater Treatment Using Conventional and Hybrid Technologies: Towards Sustainable Wastewater Reuse and Recovery. *J. Water Process Eng*. 2023, *52*, 103604. DOI: 10.1016/j.jwpe.2023.103604.

[33] Gautam, R. K.; Jaiswal, N.; Singh, A. K.; Tiwari, I. Ultrasound-Enhanced Remediation of Toxic Dyes from Wastewater by Activated Carbon-Doped Magnetic Nanocomposites: Analysis of Real Wastewater Samples and Surfactant Effect. *Environ. Sci. Pollut. Res*. 2021, *28*, 36680–36694. DOI: 10.1007/s11356-021-13256-3.

[34] Singh, A. K.; Agrahari, S.; Gautam, R. K.; Tiwari, I. A Highly Efficient NiCo2o4 Decorated G-C3N4 Nanocomposite for Screen-Printed Carbon Electrode Based Electrochemical Sensing and Adsorptive Removal of Fast Green Dye. *Environ. Sci. Pollut. Res*. 2023. DOI: 10.1007/s11356-023-30373-3.

[35] Gautam, R. K.; Singh, A. K.; Tiwari, I. Nanoscale Layered Double Hydroxide Modified Hybrid Nanomaterials for Wastewater Treatment: A Review. *J. Mol. Liq*. 2022, *350*, 118505. DOI: 10.1016/j.molliq.2022.118505.

[36] Gautam, R. K.; Tiwari, I. Humic Acid Functionalized Magnetic Nanomaterials for Remediation of Dye Wastewater Under Ultrasonication: Application in Real Water Samples, Recycling and Reuse of Nanosorbents. *Chemosphere*. 2020, *245*, 125553. DOI: 10.1016/j.chemosphere.2019.125553.

[37] Izidoro, J. D. C.; Miranda, S.; Guilhen, S. N.; Fungaro, D. A.; Wang, S. Treatment of Coal Ash Landfill Leachate Using Zeolitic Materials from Coal Combustion By-Products. *Advan. Mater. & Tech. Envir. App*. 2018, *2*, 177–186.

[38] Rudnicki, P.; Hubicki, Z.; Kołodyńska, D. Evaluation of Heavy Metal Ions Removal from Acidic Waste Water Streams. *Chem. Eng. J*. 2014, *252*, 362–373. DOI: 10.1016/j.cej.2014.04.035.

[39] Perez, I. D.; Anes, I. A.; Botelho Junior, A. B.; Espinosa, D. C. R. Comparative Study of Selective Copper Recovery Techniques from Nickel Laterite Leach Waste Towards a Competitive Sustainable Extractive Process. *Clean Eng. Technol.* 2020, *1*, 100031. DOI: 10.1016/j.clet.2020.100031.

[40] Botelho Junior, A. B.; Jiménez Correa, M. M.; Espinosa, D. C. R.; Dreisinger, D.; Tenório, J. A. S. Recovery of Cu(ii) from Nickel Laterite Leach Using Prereduction and Chelating Resin Extraction: Batch and Continuous Experiments. *Can. J. Chem. Eng.* 2019, *97*(4), 924–929. DOI: 10.1002/cjce.23306.

[41] Alves, D. A. S.; Botelho Junior, A. B.; Espinosa, D. C. R.; Tenório, J. A. S.; Baltazar, M. D. P. G. Copper and Zinc Adsorption from Bacterial Biomass - Possibility of Low-Cost Industrial Wastewater Treatment. *Environ. Technol.* 2023, *44*(16), 2441–2450. DOI: 10.1080/09593330.2022.2031312.

[42] Totten, G. E.; Mackenzie, D. S. *Handbook of Aluminum*; Eds.; In Totten, G. E. MacKenzie, D. S. 2003.

[43] Shinzato, M. C.; Hypolito, R. Solid Waste from Aluminum Recycling Process: Characterization and Reuse of Its Economically Valuable Constituents. *Waste. Manage.* 2005, *25*(1), 37–46. DOI: 10.1016/j.wasman.2004.08.005.

[44] Shabani, J. M.; Babajide, O.; Oyekola, O.; Petrik, L. Synthesis of Hydroxy Sodalite from Coal Fly Ash for Biodiesel Production from Waste-Derived Maggot Oil. *Catalysts*. 2019, *9*(12), 1–14. DOI: 10.3390/catal9121052.

[45] Makgabutlane, B.; Nthunya, L. N.; Musyoka, N.; Dladla, B. S.; Nxumalo, E. N.; Mhlanga, S. D. Microwave-Assisted Synthesis of Coal Fly Ash-Based Zeolites for Removal of Ammonium from Urine. *R.S.C. Adv.* 2020, *10*(4), 2416–2427. DOI: 10.1039/c9ra10114d.

[46] Perez, I. D.; Botelho Junior, A. B.; Aliprandini, P.; Espinosa, D. C. R. Copper Recovery from Nickel Laterite with High-Iron Content: A Continuous Process from Mining Waste. *Can. J. Chem. Eng.* 2020, *98*(4), 957–968. DOI: 10.1002/cjce.23667.

[47] Chen, T.; Zhou, Z.; Han, R.; Meng, R.; Wang, H.; Lu, W. Adsorption of Cadmium by Biochar Derived from Municipal Sewage Sludge: Impact Factors and Adsorption Mechanism. *Chemosphere*. 2015, *134*, 286–293. DOI: 10.1016/j.chemosphere.2015.04.052.

[48] Shukla, A.; Zhang, Y.-H.; Dubey, P.; Margrave, J. L.; Shukla, S. S. The Role of Sawdust in the Removal of Unwanted Materials from Water. *J. Hazard. Mater.* 2002, *95*, 137–152. DOI: 10.1016/S0304-3894(02)00089-4.

[49] Zagorodni, A. A. *Ion Exchnange Materials: Properties and Application*, First edition; Elsevier: Stockholm, 2012; XXXIII.

[50] Shahbazi, A.; Marnani, N. N.; Salahshoor, Z. Synergistic and Antagonistic Effects in Simultaneous Adsorption of Pb(ii) and Cd(ii) from Aqueous Solutions Onto Chitosan Functionalized EDTA-Silane/MGO. *Biocatal Agric. Biotechnol.* 2019, *22*, 101398. DOI: 10.1016/j.bcab.2019.101398.

[51] Botelho Junior, A. B.; de Vicente, A.; Espinosa, D. C. R.; Tenório, J. A. S. Recovery of Metals by Ion Exchange Process Using Chelating Resin and Sodium Dithionite. *Journal Of Mater. Res. & Tech.* 2019, *8*(5), 4464–4469. DOI: 10.1016/j.jmrt.2019.07.059.

[52] Awual, M. R.; Islam, A.; Hasan, M. M.; Rahman, M. M.; Asiri, A. M.; Khaleque, M. A.; Chanmiya Sheikh, M. Introducing an Alternate Conjugated Material for Enhanced Lead(II) Capturing from Wastewater. *J. Clean. Prod.* 2019, *224*, 920–929. DOI: 10.1016/j.jclepro.2019.03.241.

[53] Rahman, M. M.; Khan, S. B.; Marwani, H. M.; Asiri, A. M.; Alamry, K. A.; Rub, M. A.; Khan, A.; Khan, A. A. P.; Qusti, A. H. Low Dimensional Ni-ZnO Nanoparticles As Marker of Toxic Lead Ions for Environmental Remediation. *J. Ind. Eng. Chem.* 2014, *20*(3), 1071–1078. DOI: 10.1016/j.jiec.2013.06.044.

[54] Khan, S. B.; Rahman, M. M.; Asiri, A. M.; Marwani, H. M.; Bawaked, S. M.; Alamry, K. A. Co3O4 Co-Doped TiO2 Nanoparticles As a Selective Marker of Lead in Aqueous Solution. *New. J. Chem.* 2013, *37*(9), 2888–2893. DOI: 10.1039/c3nj00298e.

[55] Wu, Y.; Chen, J.; Liu, Z.; Na, P.; Zhang, Z. Removal of Trace Radioactive Cs+ by Zirconium Titanium Phosphate: From Bench-Scale to Pilot-Scale. *J. Environ. Chem. Eng.* 2022, *10*, 108073. DOI: 10.1016/j.jece.2022.108073.

[56] Li, J.; Han, W.; Liu, H.; Su, M.; Chen, D.; Song, G. Simultaneous Removal of Cs(i) and U(VI) by a Novel Magnetic AMP@PDA@Fe3O4 Composite. *J. Clean. Prod.* 2023, *409*, 137140. DOI: 10.1016/j.jclepro.2023.137140.

[57] Botelho Junior, A. B.; Stopic, S.; Friedrich, B.; Tenório, J. A. S.; Espinosa, D. C. R. Cobalt Recovery from Li-Ion Battery Recycling: A Critical Review. *Metals (Basel)*. 2021, *11*(12), 1999. DOI: 10.3390/met11121999.

[58] Circle Economy. *The Circularity Gap Report 2023*; 2023.